This is a peer-reviewed, accepted author manuscript of the following article:
Javadi, Y., Hasani, M., & Sadeghi, S. (2015). Investigation of clamping effect on the welding sub-surface residual stress and deformation by using the ultrasonic stress measurement and finite element method. Journal of Nondestructive Evaluation, 34, [3].
https://doi.org/10.1007/s10921-015-0277-9

Investigation of clamping effect on the welding sub-surface residual stress and deformation by using the ultrasonic stress measurement and finite element method

Yashar Javadi[1]*

[1] Department of Mechanical Engineering, Semnan Branch, Islamic Azad University, Km. 5 of Semnan-Damghan Road, Semnan, Iran.

(* Corresponding author's e-mail: yasharejavadi@yahoo.com; Tel: +98 9124402303, Fax: +98 231 335 4030.)

Mahmood Hasani[2]

[2]Department of Mechanical Engineering, Amirkabir University of Technology, 424 Hafez Ave., Tehran, Iran.

Tel: +982164543431; Fax: +982166419736; Email: Mahmoodeng82@aut.ac.ir

Seyedali Sadeghi[3]

[3]Department of Mechanical Engineering, Amirkabir University of Technology, 424 Hafez Ave., Tehran, Iran.

Tel: +982164543431; Fax: +982166419736; Email: sadeghi1368@aut.ac.ir

ABSTRACT

In this study, sub-surface residual stress and deformations, produced by the welding process, are investigated by using ultrasonic stress measurement method and finite element (FE) simulation. The FE analysis is employed to evaluate the residual stresses and deformations caused by the tungsten inert gas (TIG) welding of 304L stainless steel plates. Residual stresses obtained from the FE analysis are then used to validate results of the ultrasonic stress measurement method, which is fulfilled by employing longitudinal critically refracted (L_{CR}) waves. By using four different frequencies of ultrasonic probes, the sub-surface residual stress fields are mapped in four different depths of the examined material. Two different plates are welded with and without the use of clamp to investigate the clamping effect on the residual stress and deformation. By employing the through-thickness measurement of residual stresses, the clamping effect on the sub-surface distribution of the residual stresses is also studied. As a result, the L_{CR} ultrasonic method is accurate enough to distinguish the surface and sub-surface residual stresses in the clamped and non-clamped welding plate. Consequently, the longitudinal residual stresses have been increased by using the clamp during the welding of stainless steel plates. However, using the clamp significantly influences the amount and distribution of longitudinal residual stress in the base metal. Regarding the welding deformation results, it has been concluded that employing the clamp considerably decreases the deformations of the stainless steel plates.

Keywords: Clamping effect; Finite Element Welding Simulation; Ultrasonic Stress Measurement; Sub-Surface Stress; Welding Residual Stress; Welding Deformation.

1. Introduction

1.1. Welding residual stress and deformation

Residual stress is described as remaining stress inside the material after the manufacturing process, in the absence of any external loads or thermal gradients. The residual stresses could affect on the material properties particularly fatigue life, dimensional stability, corrosion resistance and brittle fracture leading to the serious industrial damages. The residual stress and deformation is significantly produced in the welding process, which is an essential production process in the industry. The welding residual stress and deformation are the result of non-uniform thermal expansion and solidification caused by the welding process.

The welding deformations could be simply determined by employing the dimensional measurement instruments while the residual stress measurement has been always a serious challenge for the researchers. The stress measurement methods are categorized into the destructive, semi-destructive and non-destructive techniques. The destructive and semi-destructive methods are based on measuring the strains produced by releasing the residual stresses upon material removal from the specimen. Among them, ASTM: E837 has standardized the semi-destructive hole-drilling method suggesting it as a reliable stress measurement method. Non-destructive methods including ultrasonic, X-ray diffraction, neutron diffraction and magnetic techniques normally measure some physical parameters that are related to the stress [1].

1.2. Finite element simulation of the welding process

The finite element (FE) method has increasingly been used since early 1970s in order to estimate stresses and deformations produced by the welding processes [2]. Lindgren has reviewed

development of the finite element welding simulation in three different papers: the increased complexity of the models [3], development of material modeling [4] and computational efficiency [5]. However, the majority of studies conducted before the year 2000 simulated the welding process by using two-dimensional (2D) FE models having serious limitations in prediction of the welding distortions particularly bending and buckling shrinkage (**Fig. 1**).

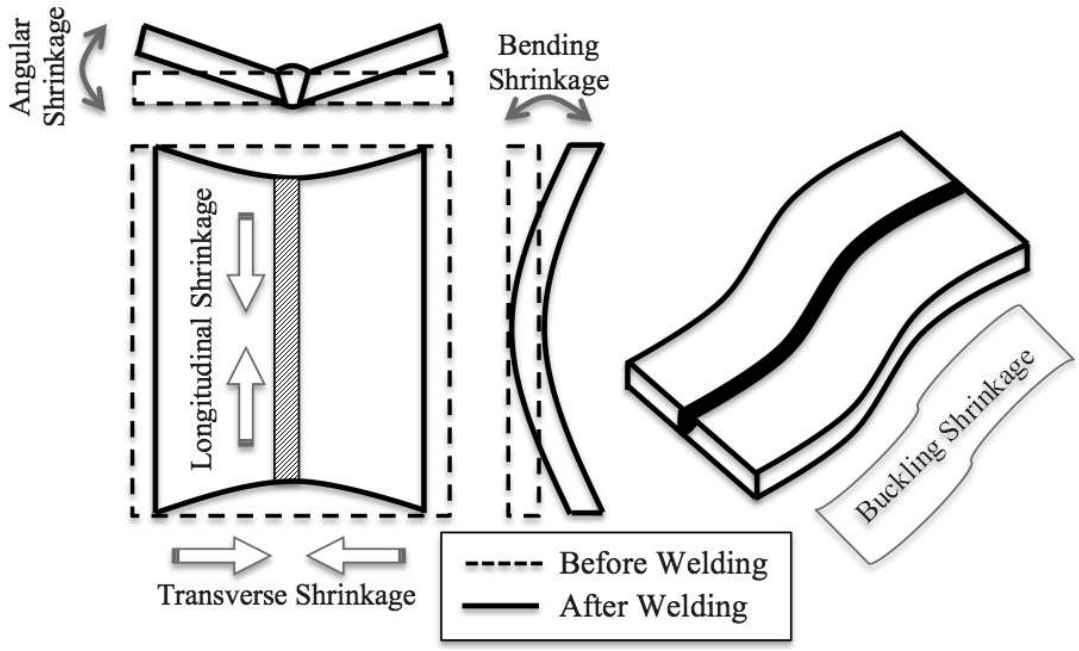

Fig. 1. The welding deformations in the plate

Recent development in the calculation capabilities of computers has motivated the researchers to analyze the residual stresses and deformations by employing three-dimensional (3D) FE models. For example, Sattari-far and Javadi [6] used a 3D-FE model to predict the welding distortions of the stainless steel pipes. They investigated the influence of welding sequence on the welding distortions concluding that the 3D model could accurately predict the welding deformations. They also showed that a significant reduction could be achieved in amount of the welding deformations by selecting the proper welding sequence.

1.3. Ultrasonic stress measurement

Ultrasonic stress measurement is a nondestructive technique based on the linear relationship between the velocity of the ultrasonic wave propagated inside the specimen and the mechanical stress of the material. The mentioned relationship is called acoustoelastic effect, which expresses that the flight time of the ultrasonic wave could vary with changing of the internal stress. Crecraft [7] proved that the acoustoelastic law could be used for stress measurement of the engineering materials. He employed the transversal ultrasonic wave; however, it was subsequently proved that longitudinal critically refracted (L_{CR}) waves are more acceptable for stress measurement. The L_{CR} wave is a longitudinal ultrasonic wave, which is propagated inside and parallel to the surface of the specimen. Egle and Bray [8] showed that the L_{CR} wave is the most sensitive ultrasonic wave to the mechanical strain and internal stress.

1.4. Sub-surface stress measurement

Among the stress measurement methods, the majority of non-destructive techniques are usually limited to near-surface depths, i.e., one or two millimeters in the steels. For instance, the conventional X-ray method is capable of measurement to a depth of about 0.02 mm [9]. However, for steels in which more penetration of wave up to 20 mm is needed, the neutron diffraction [10] and ultrasonic method could be utilized.

Bray and Tang [11] used the L_{CR} waves to measure bending stress in the steel plates. They employed two different sets of the ultrasonic probes while the testing frequencies were kept to be 2.25 MHz and 5 MHz. The comparison they made between the results of two testing frequencies enabled them to prove a unique potential of the ultrasonic method with the capability of penetration in different depth inside the specimen (by changing the excitation frequency), which provides the measurement of the bulk stress at different depths. Javadi et al [12] also confirmed

that the L_{CR} waves are able to penetrate at different depths and measure the through-thickness stresses of the material. They used four different testing frequencies of the transducers (1 MHz, 2 MHz, 4 MHz and 5 MHz) to penetrate and measure the stresses of four different depths in stainless steel plates. They also compared the ultrasonic measurement results with those obtained from the FE welding simulation. The combination of the FE analysis and stress measurement by using the L_{CR} wave was called the FEL_{CR} method, which is also considered in this study. Javadi et al [13] employed the FEL_{CR} method to evaluate the through-thickness distribution of axial and circumferential residual stresses in the stainless steel pipes. However, they proposed using another stress measurement method (like hole-drilling) to validate the residual stress results obtained by the FEL_{CR} method.

1.5. The main goal and objectives of this study

The main goal of this study is experimental measurement of the welding sub-surface residual stress and deformation in the austenitic stainless steel plates, which are welded with and without the use of a clamp, to investigate the clamping effect on the residual stress and deformation. The FE simulation of the welding process is also carried out to complete the FEL_{CR} method. The hole-drilling measurement is employed to validate the residual stress results of the FEL_{CR} method. By using four different testing frequencies (1 MHz, 2 MHz, 4 MHz and 5 MHz), the sub-surface residual stresses fields are mapped in four different depths of the examined material. The achieved results confirm reasonable resolution of the FEL_{CR} method to distinguish the clamping effect on the surface and sub-surface residual stresses. It is also concluded that the welding process of the stainless steel plate having clamp would lead to producing higher amount of residual stresses compared with the non-clamped welding. However, using the clamp seriously affects the longitudinal residual stress in the base metal and also the sub-surface

distribution of the residual stresses. By using the dimensional measurement instruments and also the FE simulation, the welding deformation is also evaluated and a considerable reduction in the angular shrinkage is observed in the clamped welding process.

2. Theoretical Background

2.1. L_{CR} method

Various experimental setups could be employed for residual stresses measurements accomplished by the L_{CR} waves. As a usual configuration, three ultrasonic transducers with the same excitation frequency are employed to produce and receive the L_{CR} wave. The transducers are normal probes working with the longitudinal wave. Javadi and Najafabadi [14] showed that there is no substantial difference between the contact and immersion ultrasonic probes employed in the ultrasonic stress measurement; hence, the contact probes are used in the experimental section of this study. To propagate the L_{CR} wave in the specimen, the longitudinal wave is excited at the first critical angle by a transmitter (sender) transducer, and then moves inside and parallel to the surface of the tested material. Two receiver transducers assembled in different distances from the sender will finally detect the wave. The reason of employing two receiver transducers is limitation of the environmental effects, e.g. ambient temperature, on the L_{CR} wave velocity. To be specific, the effect of undesired parameters (texture variation of the material located in the L_{CR} wave path, variation of the room temperature, variation of the couplant film thickness, etc.) could be decreased by employing two receivers, which allow comparative and more accurate measurements. More experimental details of the L_{CR} waves are discussed in the previous studies by Javadi et al [15-23] where they presented different experimental configurations needed to measure the longitudinal residual stresses of plates, circumferential and

axial residual stresses of pipes and pressure vessels. The relationship between the time-of-flight (TOF) measured by the L_{CR} wave and the corresponding uniaxial stress is developed by Egle and Bray [8] to be:

$$\Delta\sigma = \frac{E}{Lt_0}(t - t_0) \tag{1}$$

In Eq. (1), $\Delta\sigma$ is the stress change, E is the elastic modulus and L is the acoustoelastic coefficient (also known as the acoustoelastic constant) for the longitudinal waves propagated in the direction of the applied stress. The acoustoelastic constant could be measured by using a uniaxial tensile test on the specimens removed from the investigated material. Travel-time of the L_{CR} wave (t) is experimentally measured on the tested material while t_0 is the travel-time related to the stress-free sample. Measuring of the acoustoelastic constant along with the weld-induced change in the travel-time (t - t_0) leads to determination of the stress changes caused by the welding process.

The ultrasonic examination of the austenitic stainless steel welds is usually associated with practical difficulties such as ultrasound attenuation, beam skewing and beam scattering [24]. However, these problems are not simply observable in case of using the L_{CR} waves for stress measurement in the stainless steel specimens. The main reason could be the comparative characteristic of the L_{CR} stress measurement method. The results of this measurement technique depend on the variation of the travel-time (t - t_0). Hence, if some material induced difficulties (ultrasound attenuation, beam skewing or beam scattering) arise during the measurement of the t_0, they will repetitively happen in measurement of the t. Furthermore, the aforementioned problems could also impact the acoustoelastic constant of the stainless steel specimen which is measured as a unique coefficient in each part of the material. As a result, although the ultrasonic evaluation of the stainless steels are faced with some problems it is not considered as a serious problem in the stress measurement carried out by the L_{CR} waves.

2.2. Finite element welding simulation

A nonlinear transient analysis is used to run the finite element (FE) welding simulation, which has always been considered as a complicated and time-consuming FE problem. Employing two different thermal and mechanical analyses solves the FE problem. First, a nonlinear thermal analysis is run to find the temperature history of the entire domain. Then, the results of thermal analysis are imported into a nonlinear mechanical analysis as thermal body loads. The results of mechanical analysis would be the residual stresses and deformations, which are produced by the simulated welding process. Both of the thermal and mechanical analyses use the same geometrical model, meshing size and arrangement. ANSYS, a general-purposed FE program, is used for the analysis by employing a full Newton-Raphson iterative solution technique with a direct sparse matrix solver. The temperature and temperature dependent material properties are rapidly changed during the thermal analysis. Hence, the full Newton-Raphson technique by using the modified material properties is supposed to give more precise results.

Numerical analysis of residual stresses and deformations needs to take account of the mechanical properties of the weld. The coupling among heat transfer, microstructure evolution and thermal stresses also influences the process. From the thermo-mechanical point of view, the heat input can be considered as a volumetric or surfaced energy distribution. The fluid flow effect (which leads to homogenizing of the temperature in the molten area) can be imported by raising the thermal conductivity over the melting temperature. Heat transfers in solids are defined by the heat equation as following:

$$\rho \frac{dH}{dt} - div(k\nabla T) - Q = 0 \qquad (2)$$

$$k\nabla T.n = q(T,t) \quad \text{on} \quad \partial\Omega_q \qquad (3)$$

$$T = T_p(t) \qquad \text{on} \quad \partial\Omega_t \tag{4}$$

In Eq. (2-4), ρ, k, H, Q and T are the density, thermal conductivity, enthalpy, internal heat source and temperature respectively. In Eq. (3), n is the outward normal vector of domain $\partial\Omega$ and q is the heat flux density that could be dependent on the temperature and time to model the convective heat exchanges on the surface; and T_p is the prearranged temperature.

The heat input is represented by an internal heat source, which is simulated in the FE model by employing the double ellipsoid heat source pattern presented by Goldak and Akhlaghi [25]. The double ellipsoid model, also known as the Goldak model, is a widespread model employing two ellipsoid heat source patterns to simulate how the heating energy of the welding torch is transferred to the nodes of the FE model. The moving heat source is modelled by a user subroutine in the ANSYS.

The widespread "Element Birth and Death" technique is used to model the filler metal added during the welding process to fill the weld groove. The whole FE model is generated in the start of the analysis while all the elements demonstrating the weld metal (except those related to the tack welds) would be deactivated by assigning them a very low stiffness. During the thermal analysis, all the nodes connected to the deactivated elements (excluding those shared with the base metal) are fixed at the room temperature till the birth of the corresponding elements. Deactivated elements are reactivated successively when the welding torch arrives over them.

The mesh size is selected to be very fine near the weld zone while the size would be enlarged gradually with increasing the distance from the weld centreline (**Fig. 2**).

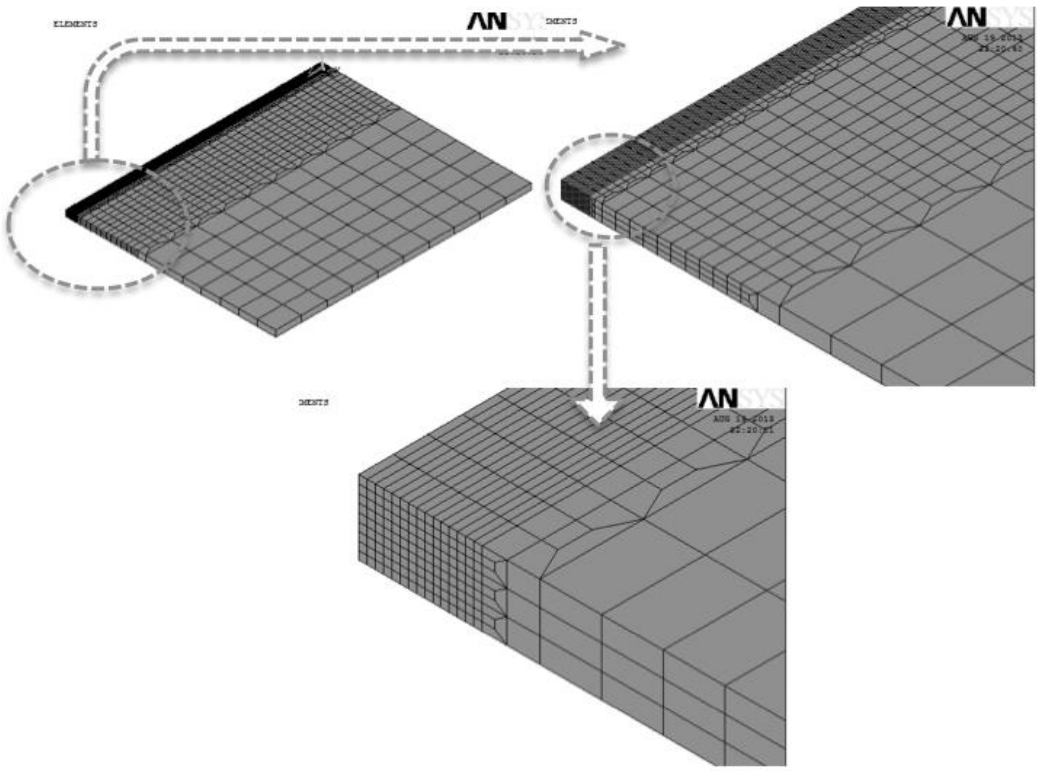

Fig. 2. The mesh size selected in the FE model

3. Experimental Procedures

3.1. Sample Description

In this study, the plates from austenitic stainless steel (304L) are welded to investigate the welding residual stresses and deformations. Two 250×200×6 mm plates are welded in V-groove (90° included angle) by utilizing the tungsten inert gas (TIG) welding process. The plates are tacked weld in two points and clamping is used during the welding process of Plate 2 (**Fig. 3**) while the Plate 1 is welded without employing the clamp. The parameters employed for the welding process of Plate 1 and Plate 2, are listed in **Table 1**.

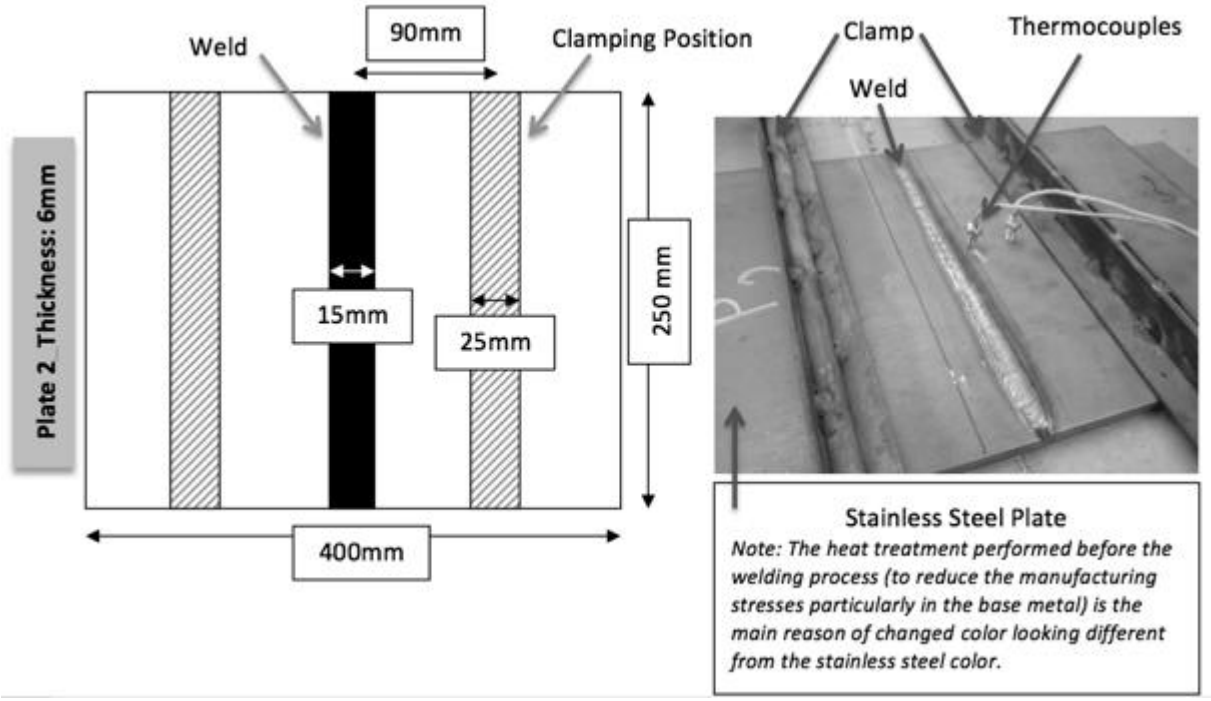

Fig. 3. The clamp position and dimensions of the Plate 2

Table 1. The welding parameters for the Plate 1&2

Sample	Pass No.	Ampere (A)	Voltage (V)	Speed (mm/s)	Clamping
Plate 1	1	120	18-19	1.94	No
	2	120	18-19	1.1	
Plate 2	1	120	18-19	1.9	Yes
	2	120	18-19	1.0	

It is not practical to test non-flat surfaces in the ultrasonic stress measurement; hence the weld reinforcement is machined by using a 30000-rpm hand grinder machine. However, a water-cooling system is employed to control the grinding temperature and avoid producing new thermal stresses.

3.2. Measurement Devices

3.2.1. Ultrasonic stress measurement

The most important part of ultrasonic stress measurement is measuring the time of flight (TOF) related to the L_{CR} wave while the required devices are shown in **Fig. 4**. TOF measurement is achieved by employing an ultrasonic portable board, laptop and ultrasonic transducers. A moving 3-axis table is also utilized to move the transducers accurately over the examined plates. The ultrasonic portable board (named as the ultrasonic box by the manufacturer) is equipped with an analogue to digital (A/D) converter, which is controlled by synchronization between the pulser signal and the internal clock. The resolution of internal clock is equal to 1 ns allowing accurate TOF measurement. To measure TOF related to the L_{CR} wave propagated in the examined material, the TOF measurement unit includes three normal ultrasonic transducers assembled in an integrated wedge. The wedge material would be poly methyl methacrylate (PMMA), under the trademark Plexiglas, which is fabricated by the laser cutting and CNC machining. The ultrasonic wave is excited at the first critical angle by the transmitter (sender) transducer, passing from the wedge and then propagates inside the material as the L_{CR} wave. Based on the Snell's law, the first critical angle related to the ultrasonic wave passing from the Plexiglas wedge and propagating in the stainless steel is calculated to be 28.2˚, which would be considered in the machining process of the wedge. Two receiver transducers assembled in different distances from the sender will finally detect the L_{CR} wave. Twelve normal transducers are prepared in four packages while the testing frequency of each package is equal to 1 MHz, 2 MHz, 4 MHz and 5 MHz. However, all the twelve transducers use the same dimensions, which is 6 mm diameter for the piezoelectric element. Using different testing frequencies is required in order to measure the bulk stresses in different depths of the plate. The pneumatic cylinder supplies a constant and

continuous pressure over the wedge to keep the thickness of the ultrasonic couplant layer constant between the wedge and examined plate.

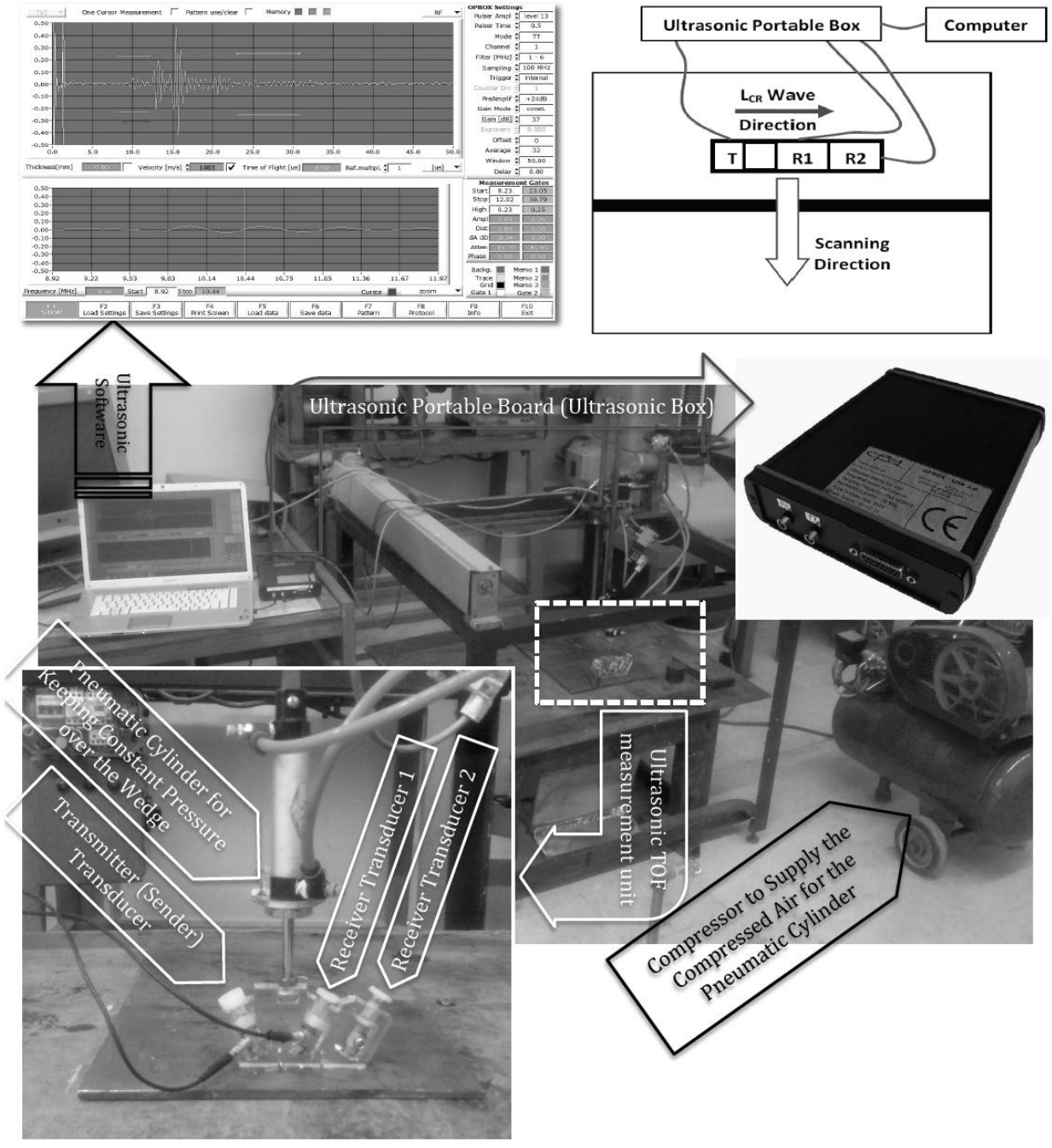

Fig. 4. The ultrasonic TOF measurement devices

When the L_{CR} wave is propagated inside the specimen, the penetration depth is expected to be a function of frequency by which the ultrasonic transducers are actuated [11]. However, the penetration depth is a wavelength effect while there is no definite relation between penetration depth of the L_{CR} wave and the frequency. Hence, the penetration depth of the L_{CR} wave needs to be measured experimentally. A variable depth groove is produced in the specimen to create a barrier in order to physically prevent the L_{CR} wave from reaching the receiver transducer. According to the measurement results, the groove with a 1 mm depth could completely prevent a 5 MHz-L_{CR} wave to pass, which indicates that the penetration depth of such a L_{CR} wave is 1 mm. Similarly, the penetration depth of 4 MHz, 2 MHz and 1 MHz-L_{CR} wave is measured 1.5 mm, 3 mm and 6 mm respectively.

According to Eq. (1), the acoustoelastic constant (L) is also needed to be measured in order to evaluate the stress. The standard uniaxial tensile test is used to measure the acoustoelastic constant based on a changed form of Eq. (1) as following:

$$L = \frac{E}{\Delta\sigma \times t_0}(t - t_0) \qquad (5)$$

By installing the TOF measurement unit on the tensile test specimens, the acoustoelastic constant could be evaluated. During the tensile test, the flight-time (t) of the L_{CR} wave would be measured while stress relief treatment is previously needed to determine the stress-free flight-time (t_0). By employing a standard tensile test machine, the tensile stress (σ) is increased step by step; meanwhile the flight-time (t) is measured in each step. The tensile test results or the material properties tables would be also used to determine the elastic modulus (E). As a result, the acoustoelastic constant (L) would be achieved based on Eq. (5).

In this study, the tensile test specimens are extracted from the weld zone and parent material (PM) to measure *E* and *L* in each of these zones. The tensile test specimens are machined according to the Sheet type (0.5 in. wide) sample presented in the ASTM: E8 standard.

3.2.2. Residual stress measurement by hole-drilling method

The residual stresses analyzed by the FE simulation are firstly needed to be verified by other reliable methods in order to validate the results obtained by the ultrasonic stress measurement. Hence, the hole-drilling standard technique is employed to verify the FE model. The hole-drilling method is carried out in five different points according to the characterizations described in ASTM: E837. The semi-destructive hole-drilling technique measures the strains relaxed by the incremental drilling of a 1.5 mm diameter hole. The strains are measured by using a strain gauge rosette after each depth increment. The residual stresses are then calculated employing equations described by ASTM: E837.

3.2.3. Measurement of the welding deformations

The welding deformations of Plate 1 and Plate 2 are measured in order to find the effect of using the clamp. Measuring the angular shrinkage (**Fig. 1**) is considered in this study. The angular shrinkage is accurately measured by employing a dial indicator gauge connected to the milling machine head while the tested plate is fixed on the milling machine table.

4. Results and Discussion

4.1. FE welding simulation

The longitudinal residual stresses analysed by the FE simulation are shown in **Fig. 5a** and **Fig. 5b** for the Plate 1 (welding without the clamp) and the Plate 2 (welding by using the clamp),

respectively. The residual stresses are shown in four different depths (0-6 mm) to describe variation of the longitudinal residual stresses through thickness of the plates. A section in the middle of the weld length, perpendicular to the weld line, is considered to analyse the residual stresses.

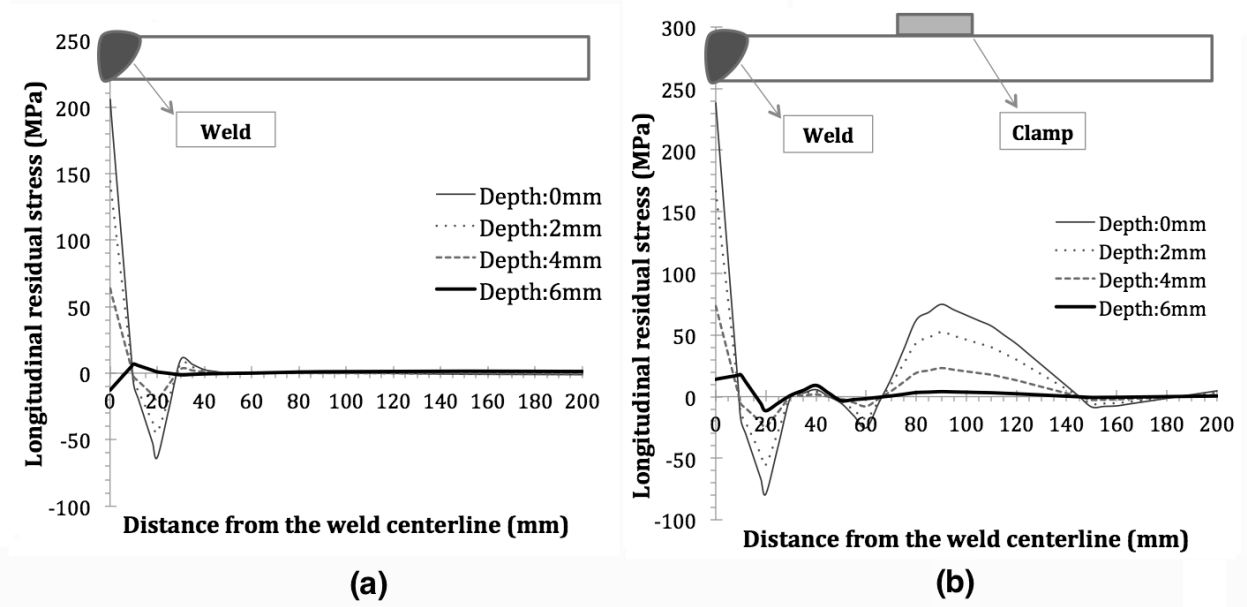

Fig. 5. The residual stress obtained from the FE analysis for (a) Plate 1 and (b) Plate 2

From the **Fig. 5**, it is generally obvious that the longitudinal residual stresses in Plate 2 experience a dramatic increase, caused by using clamp, compared with the Plate 1. To be specific, the peak of residual stress on the surface of the Plate 1 (Depth: 0 mm) is equal to 205 MPa at the weld centreline compared with 238 MPa in the Plate 2. Hence, there is an increase of about 16% in the peak of longitudinal residual stress on the surface of Plate 2 in comparison with the Plate 1.

From the **Fig. 5b**, another important effect of using the clamp could be observed which is the rising trend of residual stress between 65-90 mm distance from the weld centreline. As a normal trend of the longitudinal residual stress throughout a welded plate, the tensile stress reaches the

peak at the weld centreline, then declines sharply to reach the peak of compressive stress near the heat affected zone (HAZ), followed by a gradual rise to reach a stationary level of zero stress in the parent material (PM) zone. The aforementioned normal trend is clearly observed in the longitudinal residual stress distribution of Plate 1 surface (**Fig. 5a**, Depth: 0 mm). However, using the clamp in the Plate 2 has rocketed the amount of residual stress in the PM zone. From the **Fig. 5b** it can be observed that the growth of the residual stress in the PM zone is positioned under the clamp (the clamp is located between 77.5-102.5 mm distance from the weld centreline). The surface residual stress (Depth: 0 mm) rises from zero to 75 MPa, between 65-90 mm distance from the weld centreline, then gradually decline back to zero stress at 145 mm. Hence, using the clamp during the welding of the stainless steel plate could produce a high amount of the residual stress (up to 75 MPa or approximately one-third of the yield strength) in a specific location of the PM zone which could be a stress-free area in the absence of the clamp.

The sub-surface stresses are also considered in the **Fig. 5** by analysing the longitudinal residual stress in depths equal to 2, 4 and 6 mm. It is obvious that the longitudinal residual stresses are decreased at increasing depth. At the weld centreline of Plate 1, the longitudinal residual stress is equal to 205 MPa, 144 MPa, 64 MPa and -13 MPa for depths 0 mm, 2 mm, 4 mm and 6 mm, respectively. In addition to the downward trend of the longitudinal residual stresses at the weld centerline, a stress transformation from the tensile mode (+205 MPa) into the compressive stress (-13 MPa) is also observed in the Plate 1. However, in comparison with the surface residual stress, the bottom stress (Depth: 6 mm) is negligible and just hovering at around zero throughout the Plate 1. Similarly, the sub-surface stress analysis of the Plate 2 show a slumping trend of the longitudinal residual stresses by moving from the surface into the bottom of the plate. This trend is repeated in the locations influenced by the clamp, between 65-145 mm

distance from the weld centerline. However, the difference could be related to the bottom stress that is tensile stress at the weld centerline, in contrast with the compressive stress of the Plate 1. Hence, the clamp is able to impact on the amount and also distribution of the sub-surface residual stresses.

4.2. Validating FE model (comparing FE and hole-drilling results)

The hole-drilling measurement is employed to validate the FE model while the comparison of the mentioned methods are made on the Plate 2. The depth of hole drilled for the hole-drilling measurement is equal to 2 mm while it has been previously shown that the average of stresses in 0-2 mm depth was commonly reported by the hole-drilling method [12]. Hence, the longitudinal residual stresses achieved by the FE model (in all the nodes located in 0-2 mm depth) have to be averaged to be comparable with those obtained from the hole-drilling measurement (as shown in **Fig. 6**).

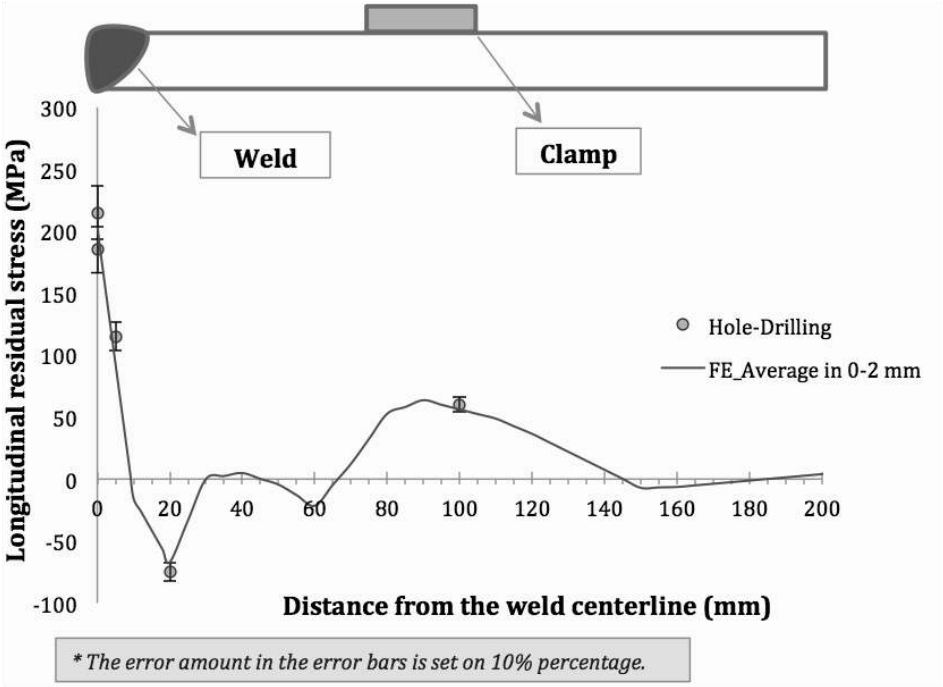

Fig. 6. Validation of the FE model by using the hole-drilling measurement

From the **Fig. 6**, it is confirmed that the difference between the FE model and hole-drilling results do not exceed 10%; hence the reasonable agreement is achieved and the FE model could be validated.

In addition to the using hole-drilling to verify mechanical results of the FE model, the results of thermal analysis (temperature history) are also validated by employing the data measured by the thermocouples which had been installed near the welding zone (**Fig. 3**).

4.3. Ultrasonic stress measurement

The validated FE model could be used to verify the results of the ultrasonic stress measurement. However, it is required to average the residual stress analyzed by the FE simulation because the L_{CR} ultrasonic method measures the average of stresses as its details are more described by Javadi et al [12-23]. To be specific, the L_{CR} ultrasonic method is not able to measure the stress in a determined depth, for instance 6 mm. Instead, the average of stress throughout 0 to 6 mm depth would be measured by the L_{CR} technique.

The comparison between the residual stresses measured by the ultrasonic method with those obtained from the FE analysis of Plate 1 and Plate 2 are shown in **Fig. 7** and **Fig. 8**, respectively.

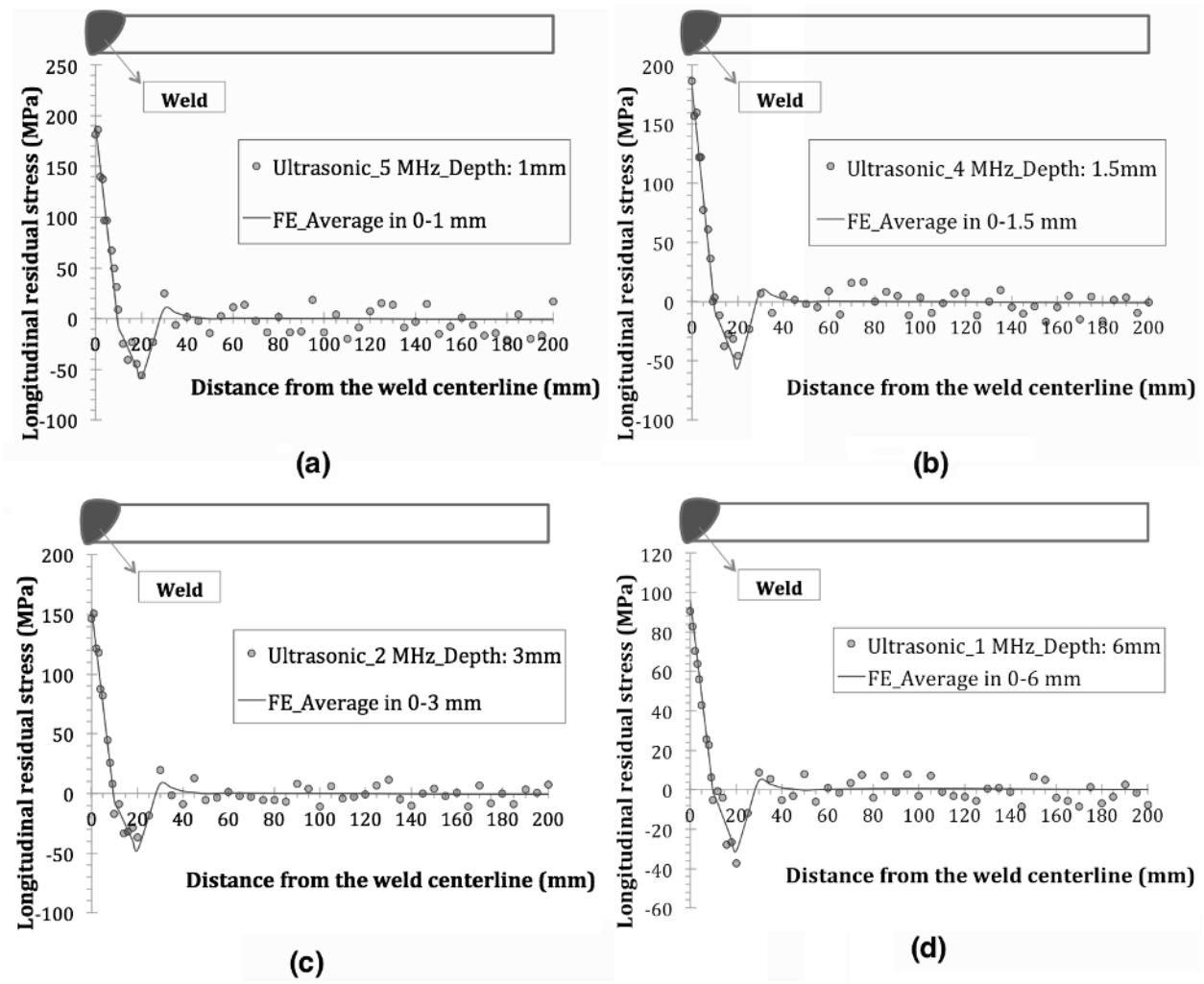

Fig. 7. Comparison between the residual stress analyzed by the FE model of Plate 1 and those obtained from the ultrasonic stress measurement fulfilled by using (a) 5 MHz, (b) 4 MHz, (c) 2 MHz and (d) 1 MHz transducers

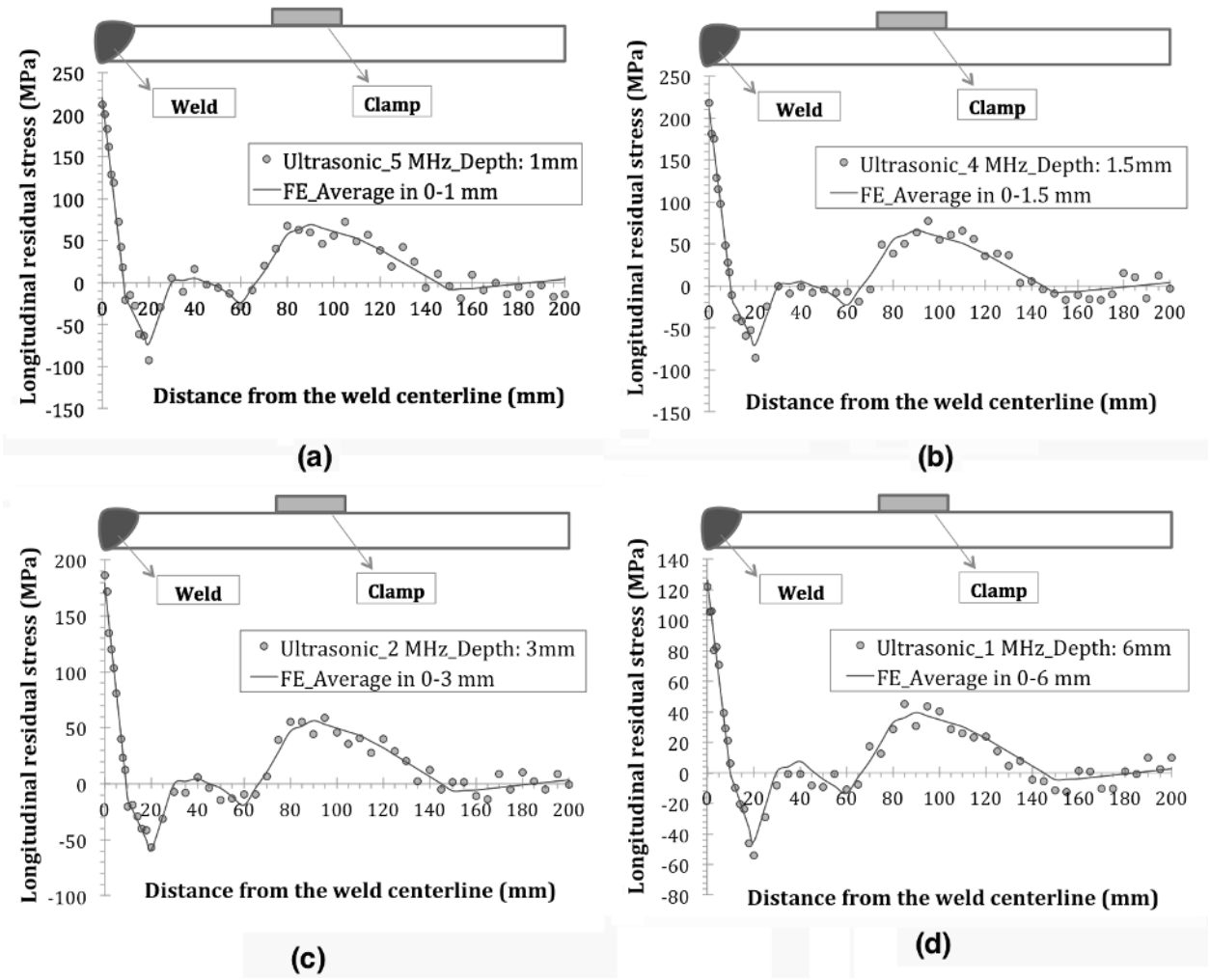

Fig. 8. Comparison between the residual stress analyzed by the FE model of Plate 2 and those obtained from the ultrasonic stress measurement fulfilled by using (a) 5 MHz, (b) 4 MHz, (c) 2 MHz and (d) 1 MHz transducers

There is a reasonable agreement (as shown in the **Fig. 7** and **Fig. 8**) between the FE and ultrasonic results related to the longitudinal residual stresses. The maximum and average of the differences achieved between the residual stresses analysed by the FE model with those obtained from the ultrasonic stress measurement, are listed in **Table 2**.

Table 2. The maximum and average of differences achieved between the results of the FE and ultrasonic

	Plate 2 (Clamp Welding)				Plate 1 (No-Clamp)			
Depth in which the FE analysis and ultrasonic measurement results are compared (mm)	0-1	0-1.5	0-3	0-6	0-1	0-1.5	0-3	0-6
Maximum of differences achieved between the longitudinal residual stress analyzed by the FE model with those measured by the ultrasonic method (MPa)	20	17	12	10	20	17	12	9
Average of differences achieved between the longitudinal residual stress analyzed by the FE model with those measured by the ultrasonic method (MPa)	9	9	6	6	11	8	6	4

From the **Table 2**, it can clearly be seen that the maximum difference between the FE and ultrasonic results, related to the longitudinal residual stress, is equal to 20 MPa, which is about 10% of the yield strength of the stainless steel plate. Hence, the reasonable agreement is achieved between the results of the FE model with those achieved by the ultrasonic stress measurement. The aforementioned agreement confirms the FEL_{CR} potential in the stress evaluation of the stainless steel plates welded with and without using the clamp. However, the FEL_{CR} potential in stress evaluation of the stainless steel plates was previously confirmed by Javadi et al [12] but the capability of this method in recognizing the stress change made by using clamp, was under question. According to the results shown in **Fig. 7** and **Fig. 8** as well as **Table 2**, the resolution of the L_{CR} method is suitable enough to measure the influence of using the clamp on the longitudinal residual stresses of the stainless steel plates.

4.4. Deformation measurement results

The measurement results of angular shrinkages in the Plate 1&2 are compared in **Fig. 9**. It is obvious that the clamping could lead to reduction of the welding deformations. From the **Fig. 9**,

the welding angular shrinkage of the Plate 1 reaches about 10 mm, whereas this value is only 1 mm for the plate 2.

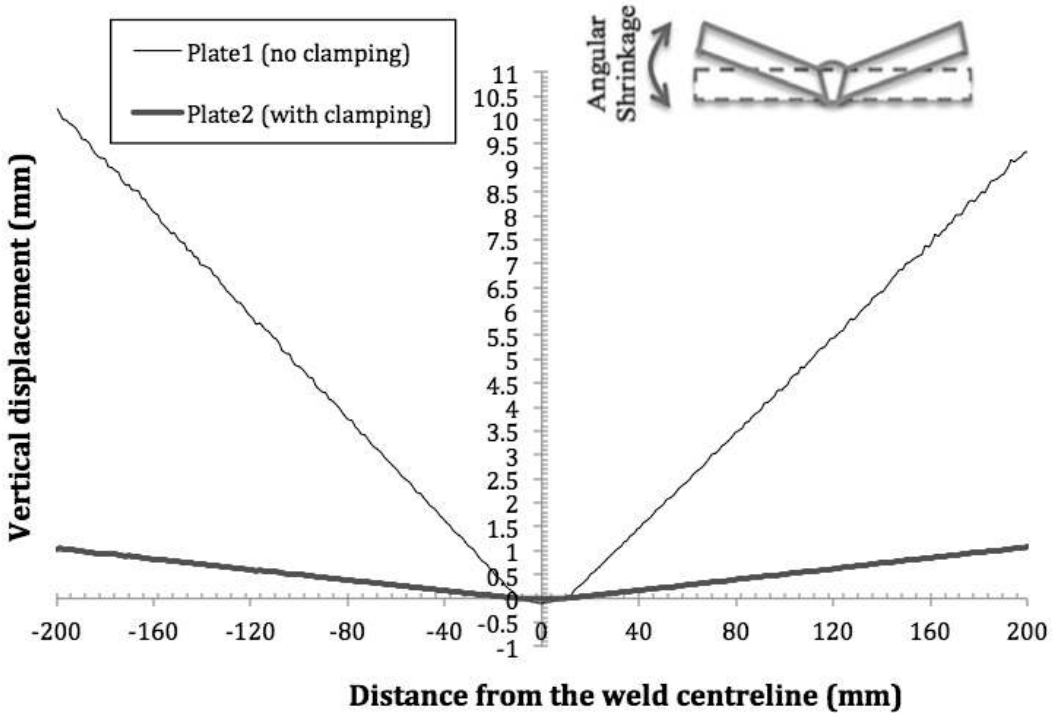

Fig. 9. Clamping effect on the welding deformations

It was expected to reach lower deformations by employing the clamp welding which is considered as a simple practical method to control the welding deformations. However, comparing the clamp effect on the welding deformation and residual stresses could be instructive. Using the clamp could decrease the angular shrinkages to one tenth of non-clamp welding case while about 16% increase in the longitudinal residual stresses would be achieved by using the clamp. Furthermore, using the clamp could impact the sub-surface residual stresses and also change of the longitudinal stress distribution particularly in the PM zone. Hence, the sub-surface residual stresses and also the residual stress distribution throughout the PM zone is

required to be considered, as well as the amount of the welding deformations and residual stresses to comprehensively investigate the clamping effect in the welding processes.

5. Conclusions

The main goal of this study is evaluation of the sub-surface residual stresses and deformation in the stainless steel plates to investigate the effect of using clamp on the welding residual stresses and deformations. The FEL_{CR} method (which is the combination of finite element welding simulation with the L_{CR} ultrasonic stress measurement), hole-drilling method and angular shrinkage measurement are employed to reach this goal. According to the achieved results, it can be concluded that:

1) There is an increase of about 16% in the peak of the longitudinal residual stress on the surface of the clamped plate compared with the no-clamp welding case.
2) Using the clamp during the welding of the stainless steel plate could produce high amount of residual stress (up to 75 MPa) in the PM zone while there is a stress-free area in the absence of the clamp.
3) Using the clamp influences the amount and also the distribution of the sub-surface residual stresses.
4) The resolution of L_{CR} method is suitable enough to distinguish the influence of using the clamp on the longitudinal residual stresses of the stainless steel plates.
5) Using the clamp could decrease the angular shrinkage of the specimen to one tenth of the non-clamp welding case.

According to the results achieved in this study, in an industrial welding case which employing the clamp is under question, it is recommended to simultaneously consider the influences of

using clamp on the (i) amount of welding deformations, (ii) amount of residual stresses in the weld zone, (iii) amount and distribution of sub-surface residual stresses and (iv) residual stress distribution throughout the PM zone.

References

[1] Rossini NS, Dassisti M, Benyounis KY, Olabi AG (2012) Methods of measuring residual stresses in components. J Materials & Design 35:572-588.

[2] Hibbit HD, Marcal PV (1973) A numerical thermo-mechanical model for the welding and subsequent loading of a fabricated structure. Comput Struct 3: 1145–74.

[3] Lindgren LE (2001) Finite element modeling of welding, Part 1: Increased complexity. J Therm Stresses 24: 141–92.

[4] Lindgren LE (2001) Finite element modeling of welding, Part 2: Improved material modeling. J Therm Stresses 24: 195–231.

[5] Lindgren LE (2001) Finite element modeling of welding, Part 3: Efficiency and integration. J Therm Stresses 24: 305–34.

[6] Sattari-Far I, Javadi Y (2008) Influence of welding sequence on welding distortions in pipes. Int J of Pressure Vessels and Piping 85:265–274.

[7] Crecraft DI (1967) The Measurement of Applied and Residual Stresses in Metals Using Ultrasonic Waves. J Sound Vib 5: 173-92.

[8] Egle DM, Bray DE (1976) Measurement of Acoustoelastic and Third-Order Elastic Constants for Rail Steel. J Acoust Soc Am 60:741-744.

[9] Noyan IC, Cohen JB (1987) Residual stresses measurement by diffraction and interpretation. Berlin: Springer.

[10] Withers PJ, Webster PJ (2001) Neutron and synchrotron X-ray strain scanning. Strain 2001 37:19–33.

[11] Bray DE, Tang W (2001) Subsurface stress evaluation in steel plates and bars using the LCR ultrasonic wave. Nucl Eng Des 207: 231-40.

[12] Javadi Y, Akhlaghi M, Najafabadi MA (2013) Using Finite Element and Ultrasonic Method to Evaluate Welding Longitudinal Residual Stress through the Thickness in Austenitic Stainless Steel Plates. J Mater Des 45: 628–42.

[13] Javadi Y, Pirzaman HS, Raeisi MH, Najafabadi MA (2013) Ultrasonic inspection of a welded stainless steel pipe to evaluate residual stresses through thickness. J Mater Des 49: 591–601.

[14] Javadi Y, Ahmadi Najafabadi M (2013) Comparison between contact and immersion ultrasonic method to evaluate welding residual stresses of dissimilar joints. J Mater Des 47: 473–82.

[15] Javadi Y, Najafabadi MA, Akhlaghi M (2013) Comparison between Contact and Immersion Method in Ultrasonic Stress Measurement of Welded Stainless Steel Plates. J Test Eval 41: 1-10.

[16] Javadi Y, Pirzaman HS, Raeisi MH, Najafabadi MA (2013) Ultrasonic Evaluation of Welding Residual Stresses in Stainless Steel Pressure Vessel. J Pressure Vessel Technol 135 (041502): 1-6.

[17] Javadi Y, Najafabadi MA, Akhlaghi M (2012) Residual Stress Evaluation in Dissimilar Welded Joints Using Finite Element Simulation and the LCR Ultrasonic Wave. Russ J Nondestr Test 48: 541–52.

[18] Javadi Y, Afzali O, Raeisi MH, Najafabadi MA (2013) Nondestructive Evaluation of Welding Residual Stresses in Dissimilar Welded Pipes. J Nondestr Eval 32: 177-87.

[19] Javadi Y, Akhlaghi M, Najafabadi MA (2013) Nondestructive Evaluation of Welding Residual Stresses in Austenitic Stainless Steel Plates. Res Nondestr Eval 25: 30-40.

[20] Sadeghi S, Najafabadi MA, Javadi Y, Mohammadisefat M (2013) Using ultrasonic waves and finite element method to evaluate through-thickness residual stresses distribution in the friction stir welding of aluminum plates. J Mater Des 52: 870-80.

[21] Javadi Y (2013) Ultrasonic Measurement of Hoop Residual Stress in Stainless Steel Pipes. J Manuf Ind Eng 1–2: 1–6.

[22] Javadi Y, Hloch S (2013) Employing the LCR Waves to Measure Longitudinal Residual Stresses in Different Depths of a Stainless Steel Welded Plate. Adv Mater Sci Eng 2013: 746187.

[23] Javadi Y, Sadeghi S, Najafabadi MA (2013) Taguchi optimization and ultrasonic measurement of residual stresses in the friction stir welding. J Mater Des 55: 27–34.

[24] Kapranos PA, Whittaker VN (1983) Difficulties in the ultrasonic inspection of 316 austenitic steel welds arising from acoustic impedance mismatch. Nondestructive testing and evaluation 1: 81-92.

[25] Goldak J, Akhlaghi M (2005) Computational welding mechanics. Springer.

Figure1
Click here to download high resolution image

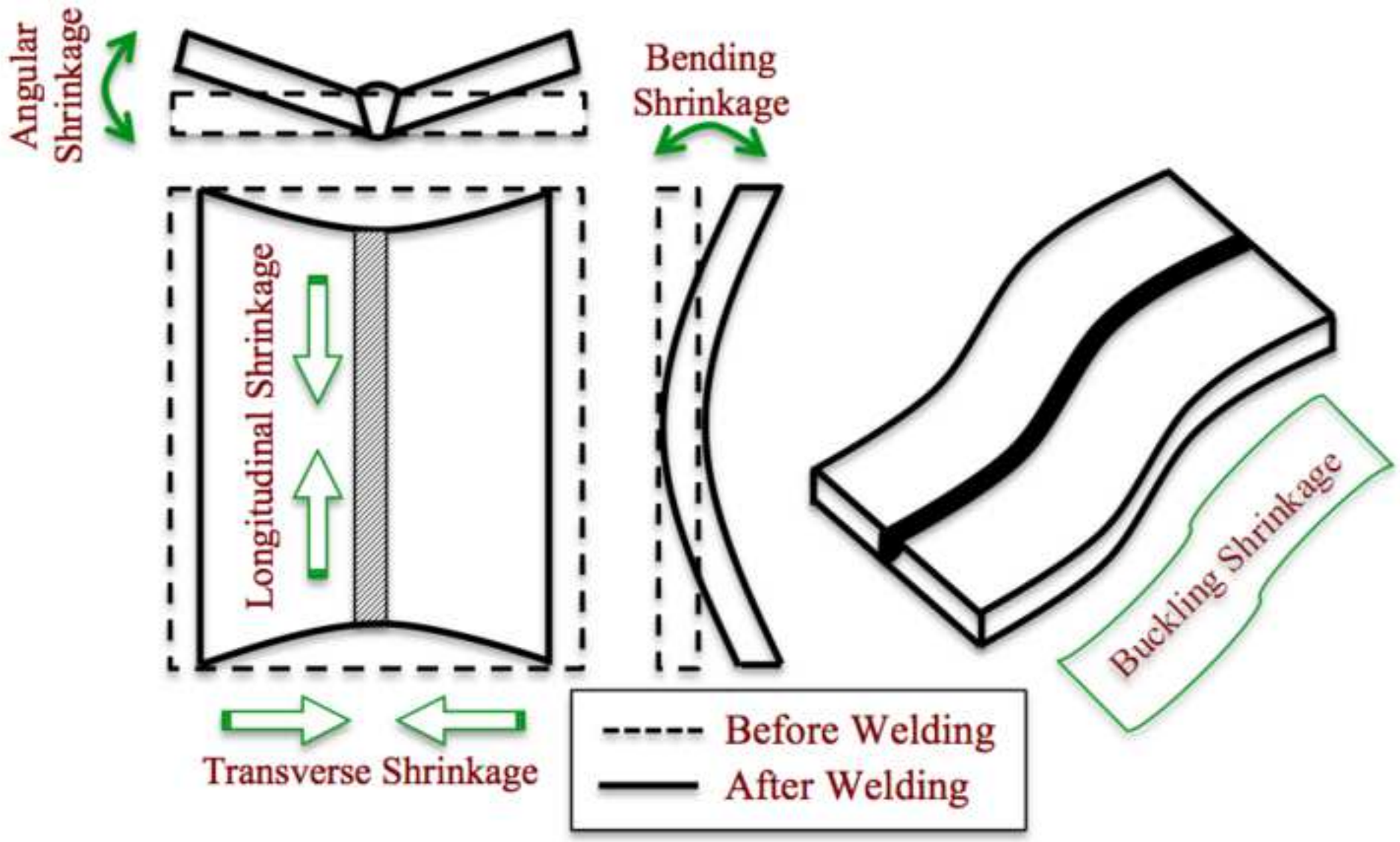

Figure2
Click here to download high resolution image

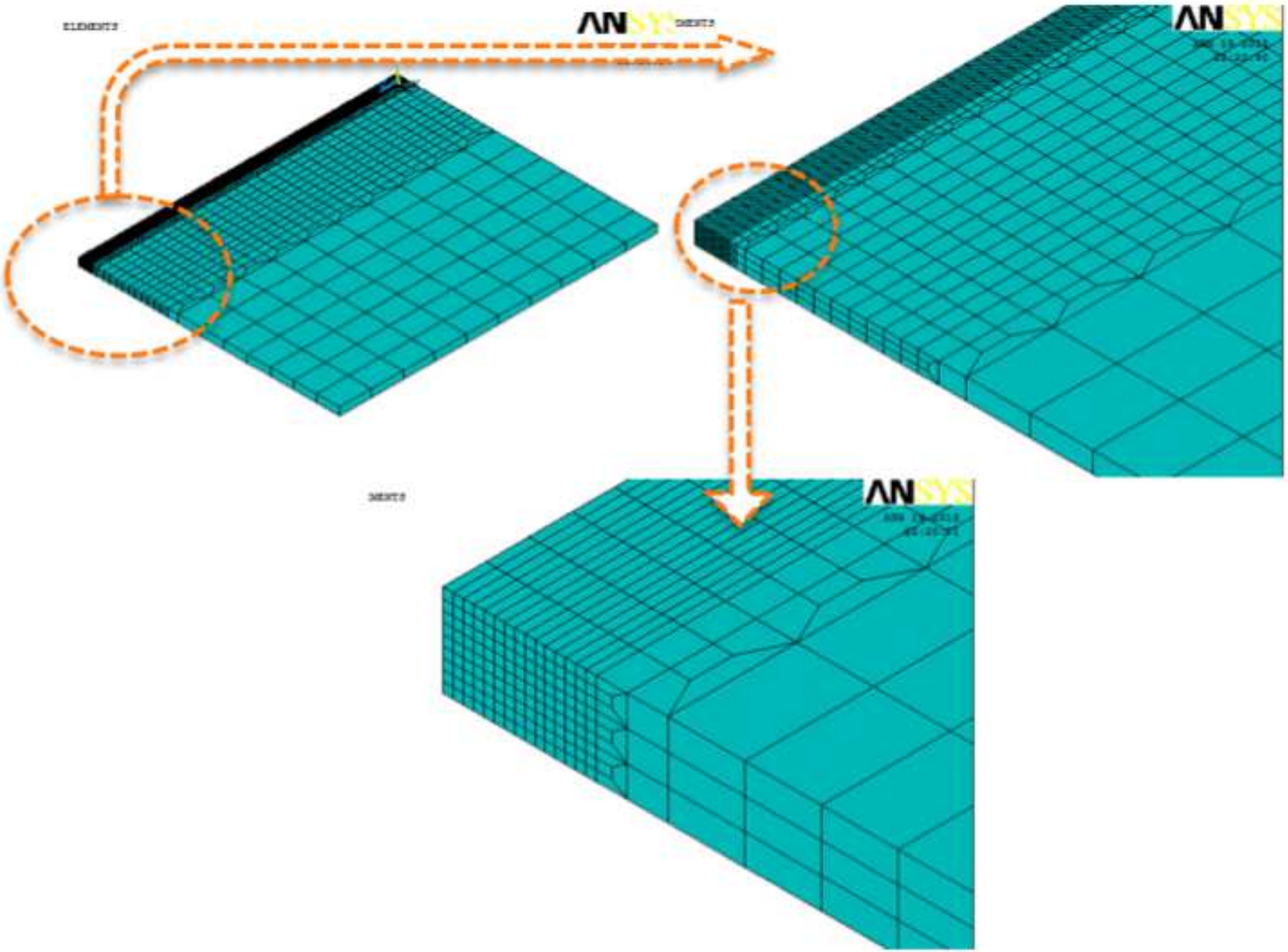

Figure3
Click here to download high resolution image

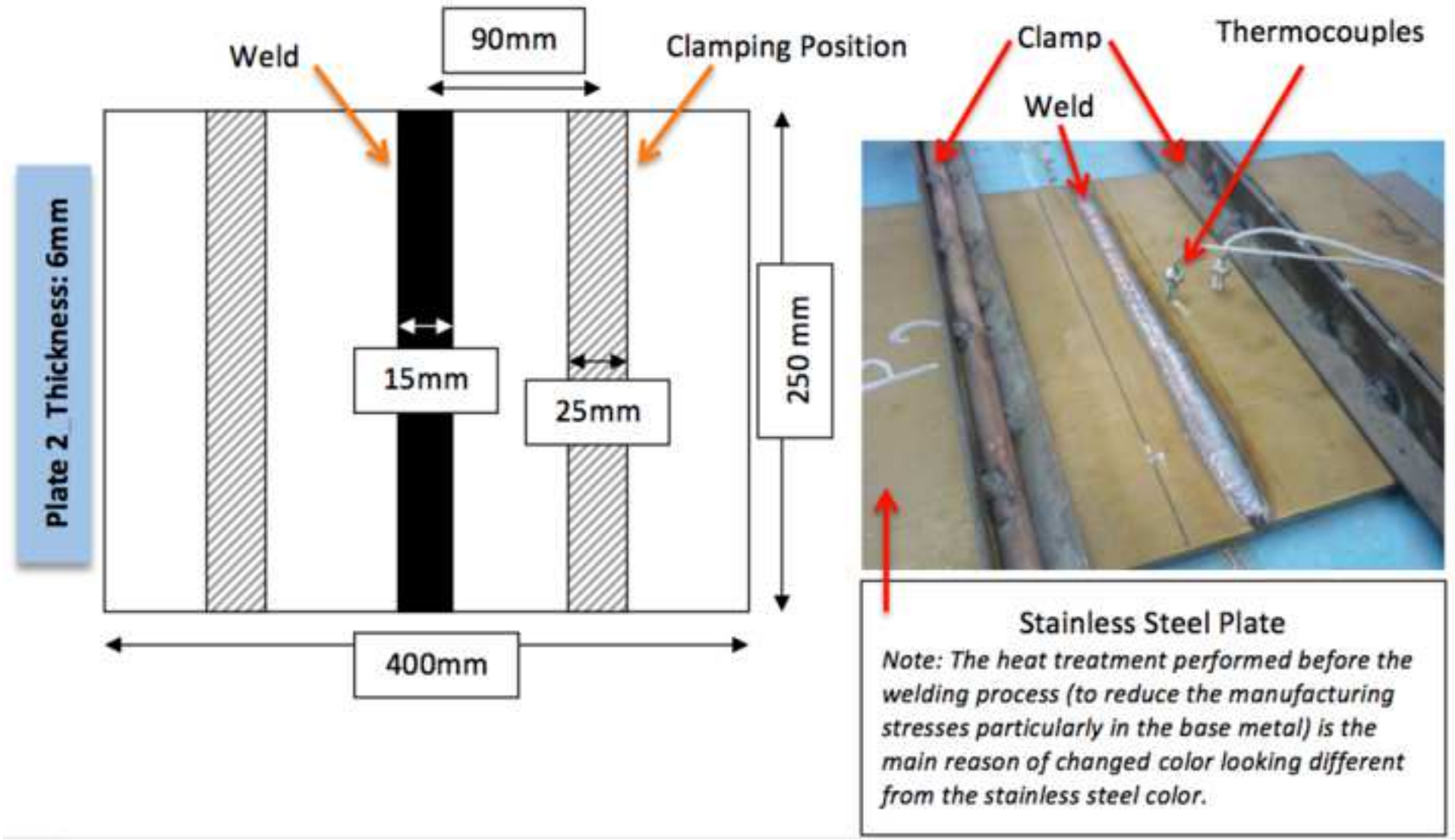

Figure4
Click here to download high resolution image

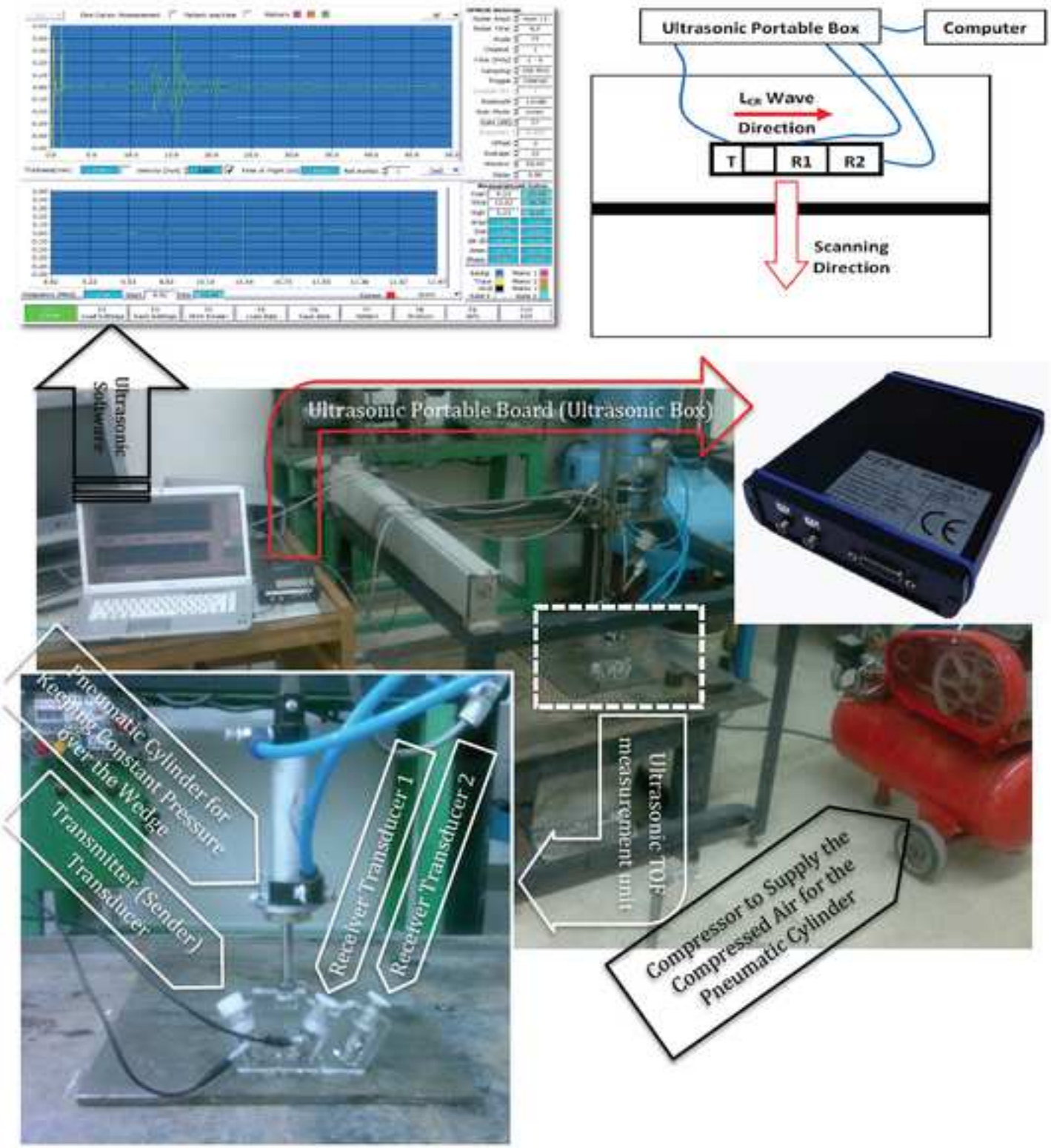

Figure5
Click here to download high resolution image

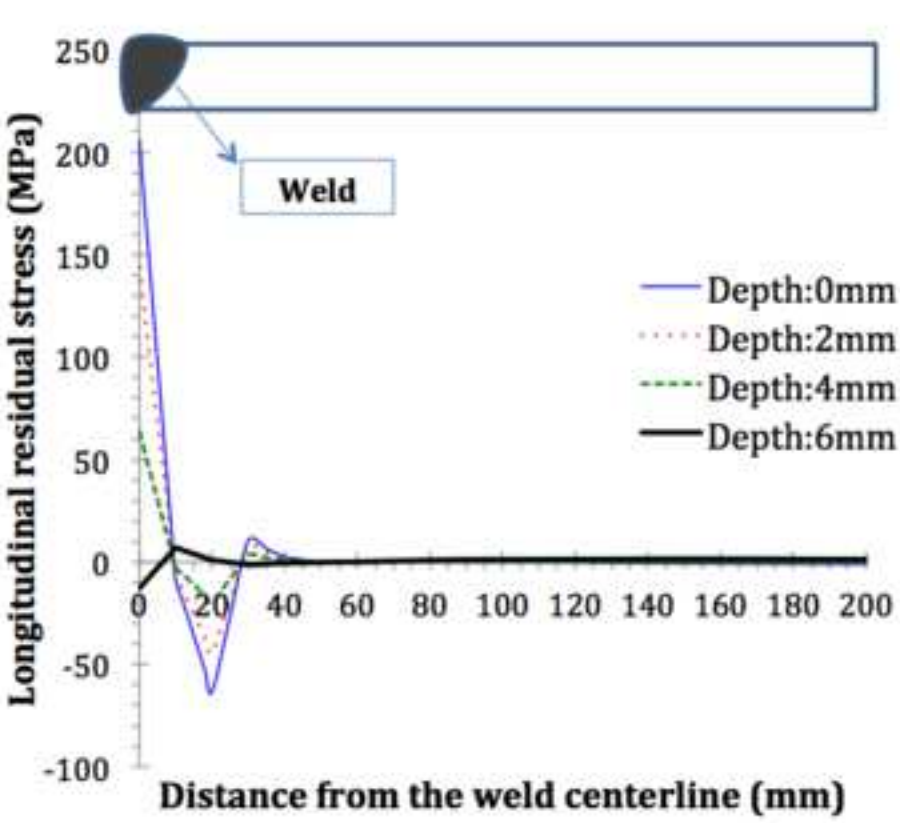

(a)

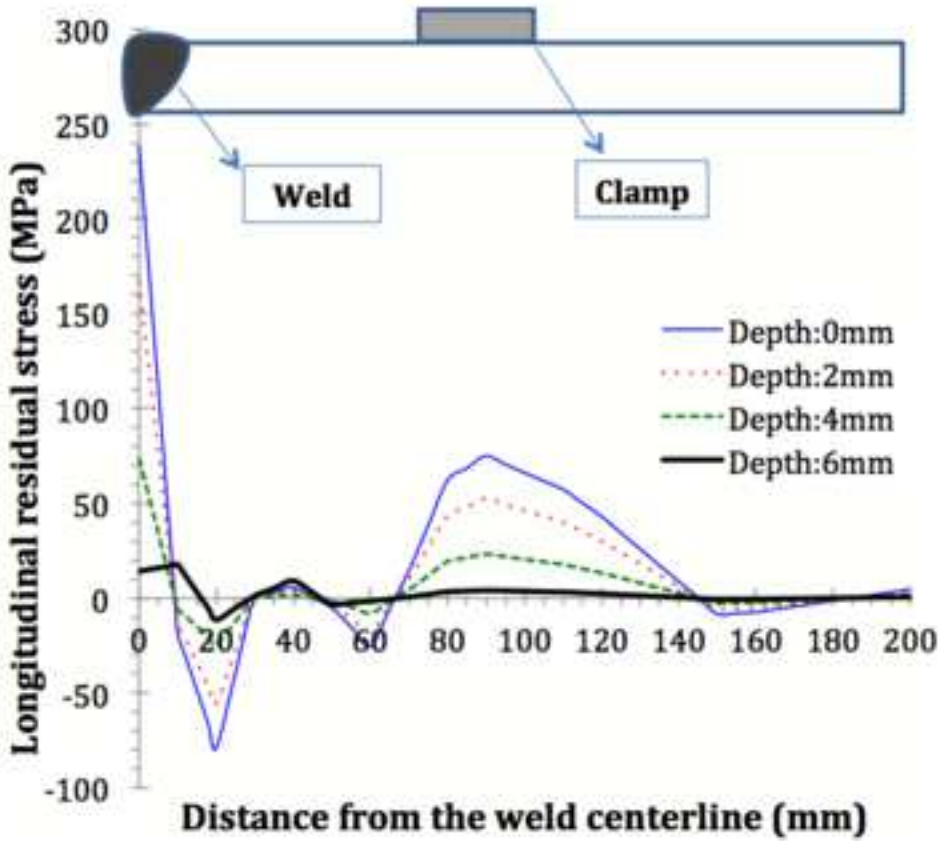

(b)

Figure6
Click here to download high resolution image

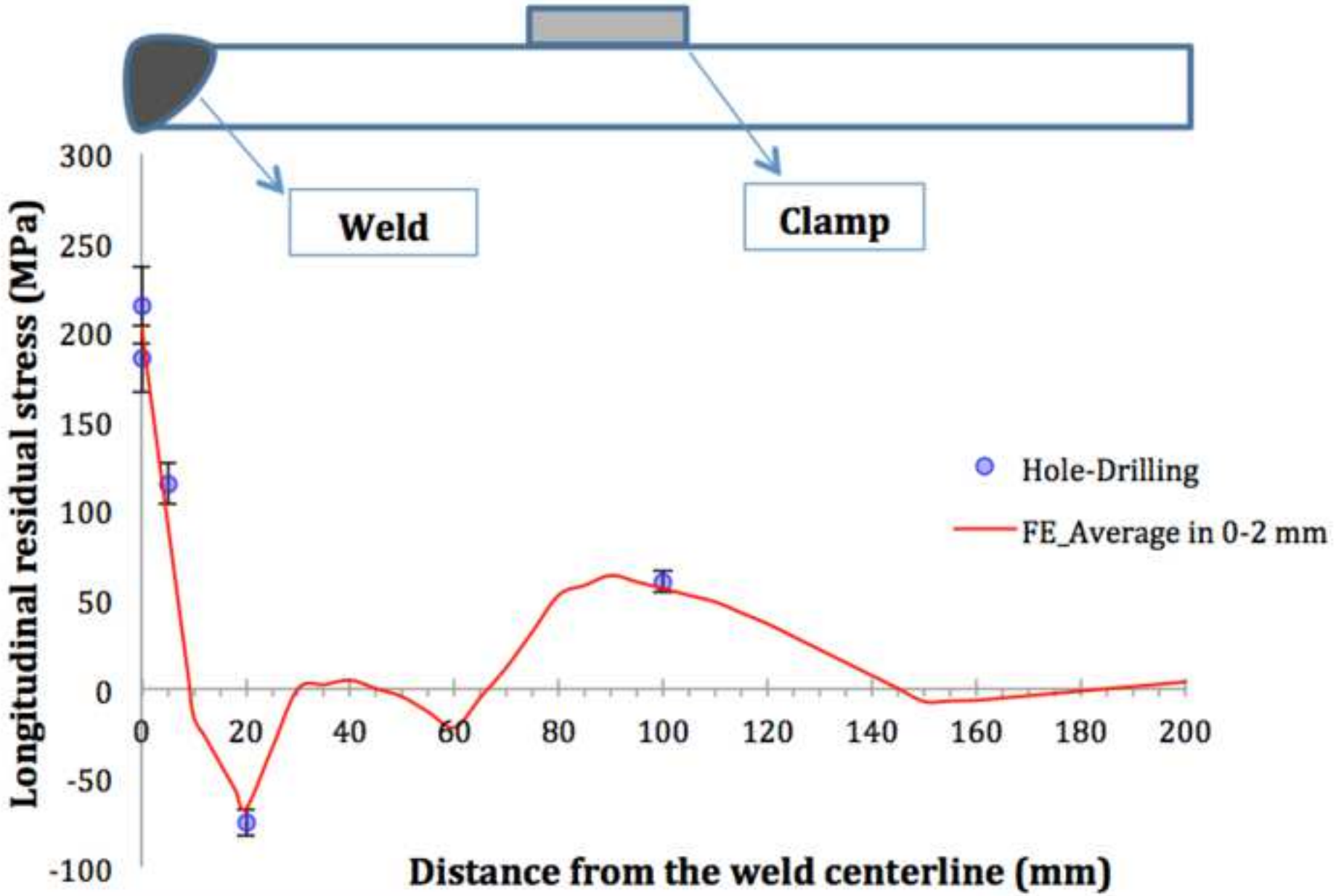

Figure7
Click here to download high resolution image

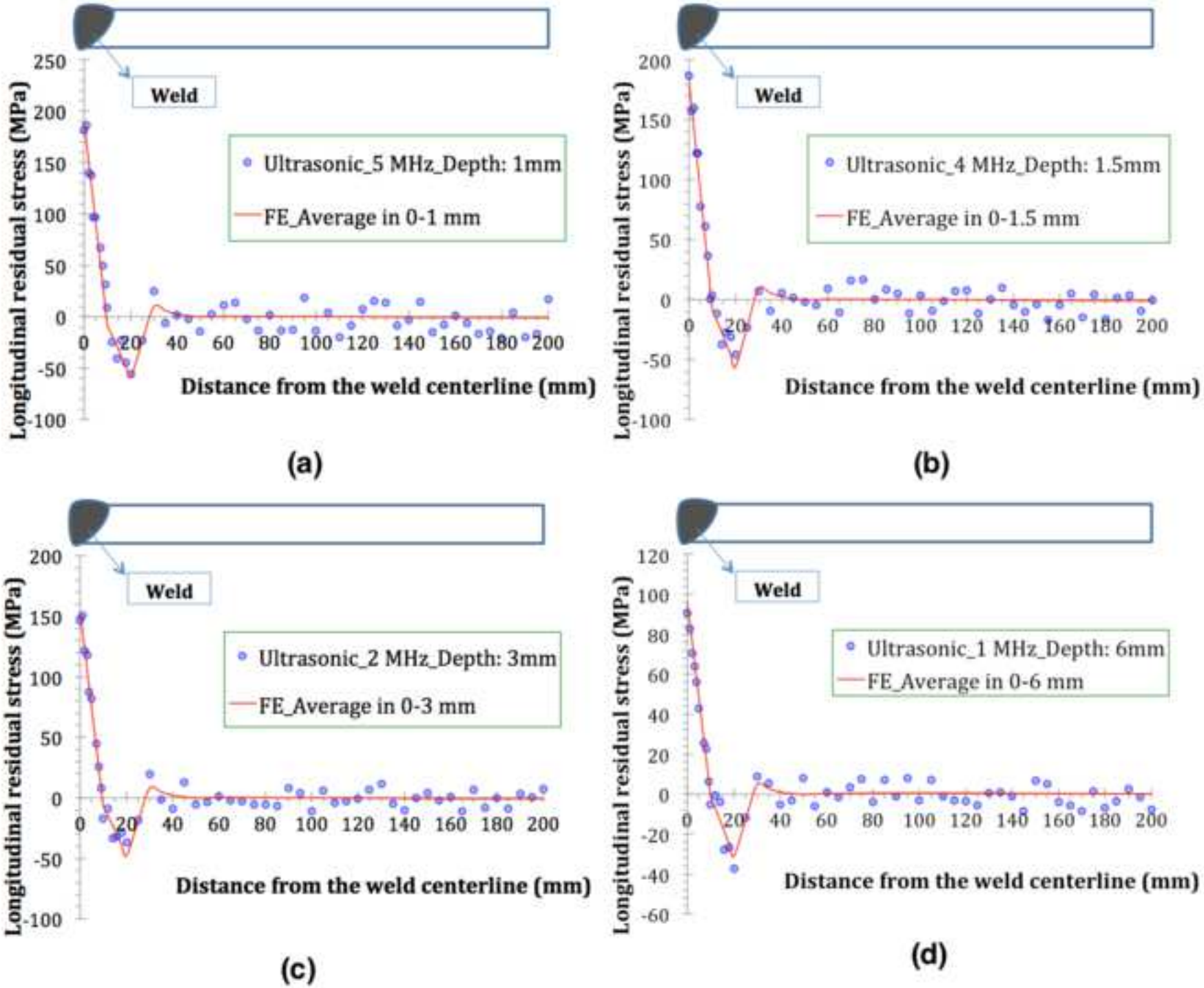

Figure8
Click here to download high resolution image

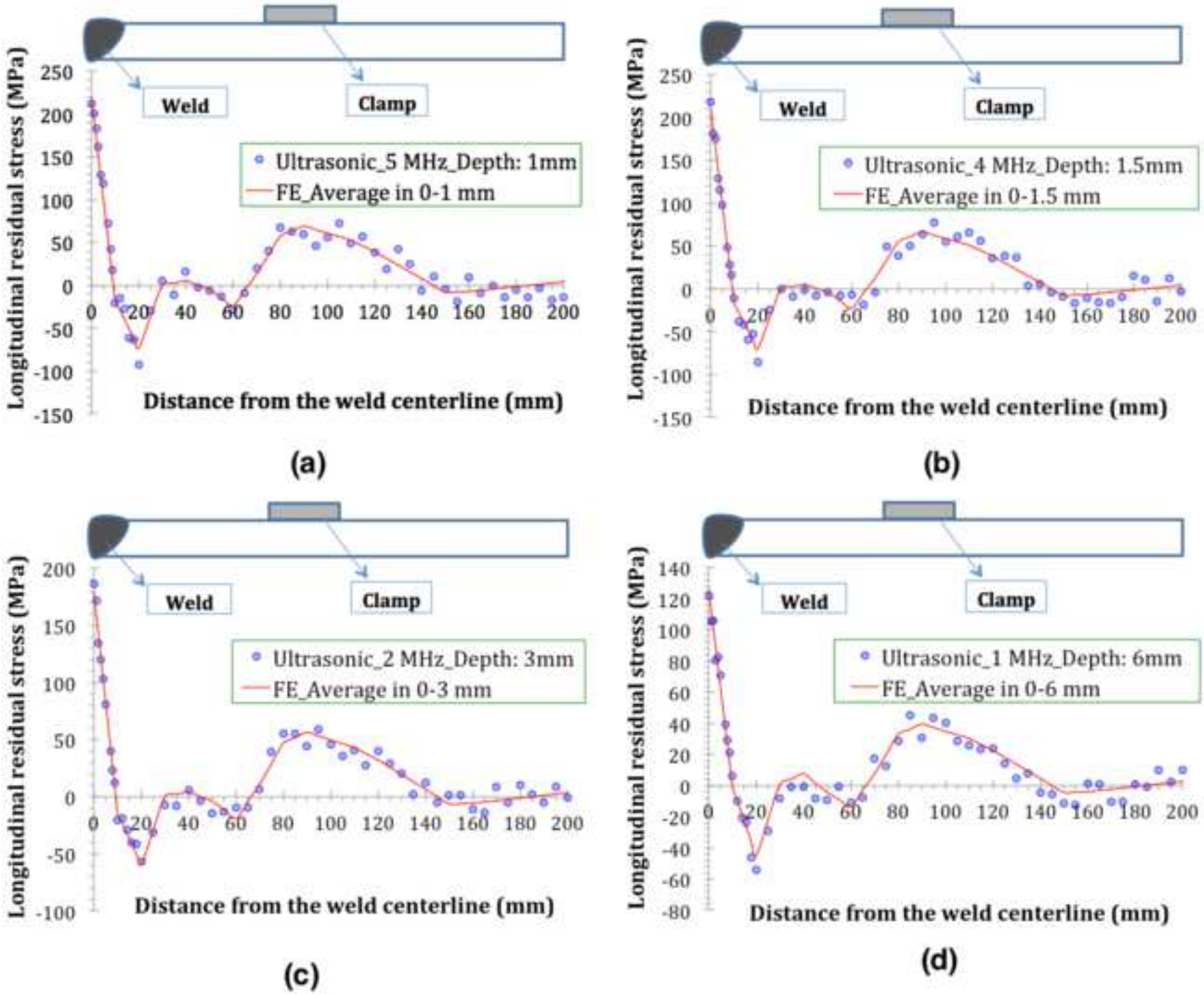

Figure9
Click here to download high resolution image

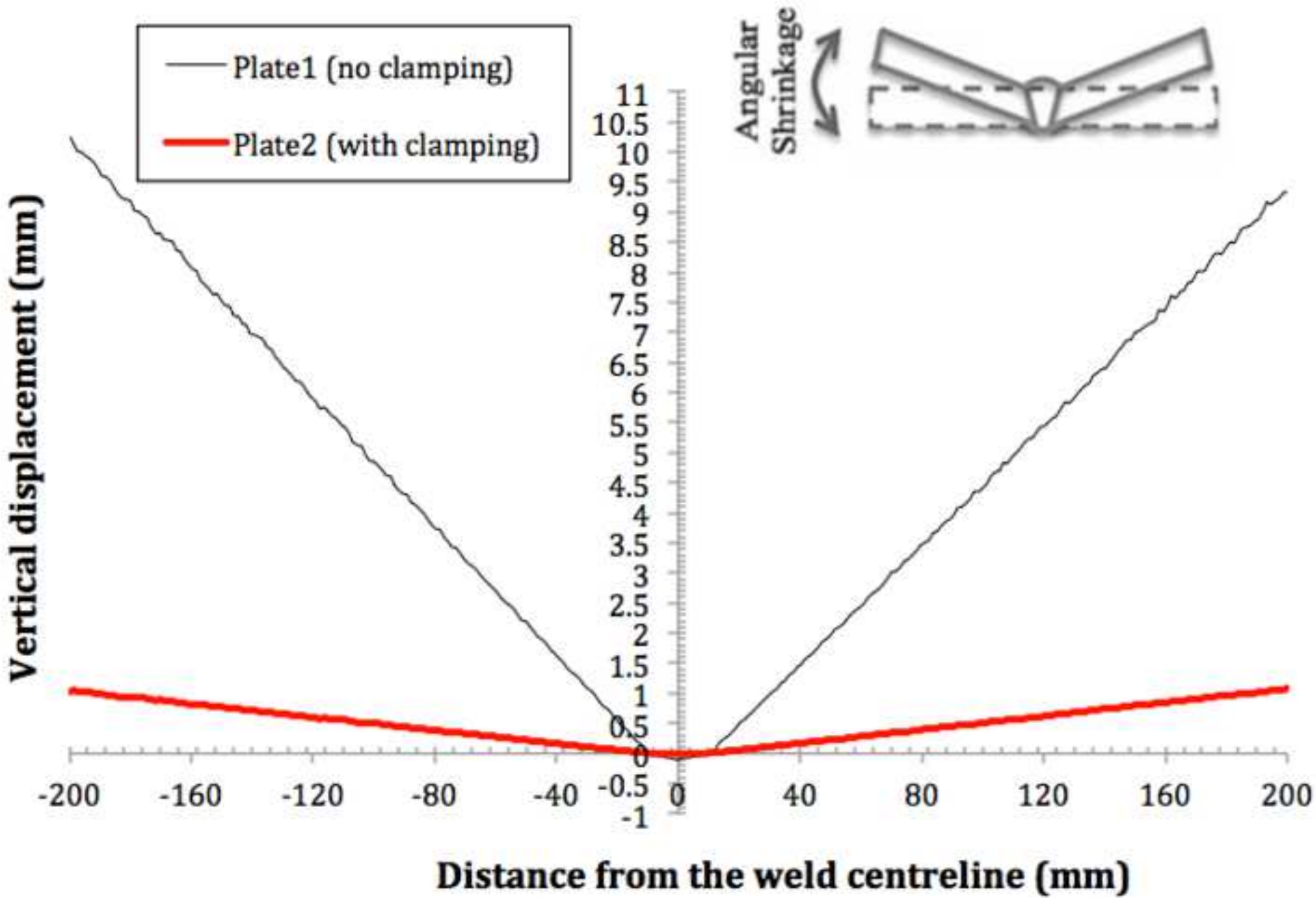

Table
Click here to download Table: Tables.docx

Table 1. Welding parameters for Plate 1&2

Sample	Pass No.	Ampere (A)	Voltage (V)	Speed (mm/s)	Clamping
Plate 1	1	120	18-19	1.94	No
	2	120	18-19	1.1	
Plate 2	1	120	18-19	1.9	Yes
	2	120	18-19	1.0	

Table 2. The maximum and average of differences achieved between the results of FE and ultrasonic

	Plate 2 (Clamp Welding)				Plate 1 (No-Clamp)			
Depth in which the FE analysis and ultrasonic measurement results are compared (mm)	0-1	0-1.5	0-3	0-6	0-1	0-1.5	0-3	0-6
Maximum of differences achieved between the longitudinal residual stress analyzed by the FE model with those measured by the ultrasonic method (MPa)	20	17	12	10	20	17	12	9
Average of differences achieved between the longitudinal residual stress analyzed by the FE model with those measured by the ultrasonic method (MPa)	9	9	6	6	11	8	6	4